Supplementary Data

Damage Recognition Models in Prokaryotic Nucleotide Excision Repair: Benzo[*a*]pyrene-Derived Lesions in UvrB

Lei Jia[‡], *Konstantin Kropachev*[§], *Shuang Ding*[‡], *Bennett Van Houten*[¶], *Nicholas E. Geacintov*[§], *and Suse Broyde*[‡, §, *]

[‡] Department of Biology and [§] Department of Chemistry, New York University,100 Washington Square East, Room 1009, New York, New York 10003, [¶] Laboratory of Molecular Genetics, National Institute of Environmental Health Sciences, National Institutes of Health, 111 TW Alexander Drive, Research Triangle Park, North Carolina 27709

Running title: Damage recognition in UvrB

Key words: Nucleotide Excision Repair; UvrB; Flip Out; Translocation

[*]To whom correspondence should be addressed: Suse Broyde: tel. (212)998-8231, fax (212)995-4015, e-mail broyde@nyu.edu

Molecular dynamics protocol

The system was reoriented with SIMULAID (1) to minimize the number of water molecules needed for solvation. The LEaP module of AMBER 8.0 was then employed to add counterions for neutralization and to solvate with a rectangular box of TIP3P water molecules (2). A buffer distance of 10Å between each wall and the closest solute atom in each direction was employed. The number of counterions and water molecules added to the system and the sizes of the solvation boxes are given in Table S5.

All systems followed the same equilibration and MD treatment: (1) minimization of the counterions and solvent molecules (including crystallized waters) for 2000 steps of SD followed by 3000 steps of CG with 50 kcal/mol restraints on the solute atoms; (2) 30 ps initial MD at 10 K with 25 kcal/mol restraints on solute molecules allowing the solvent to relax; (3) 80 ps constant volume MD simulation to heat the system up from 10 K to 328 K followed by 20 ps constant volume MD at 328 K with 10.0 kcal/mol restraints on solute molecules; (4) 30 ps, 40 ps, and 50 ps MD with decreasing restraints of 10.0, 1.0, and 0.1 kcal/mol, respectively, on solute molecules; (5) 5 ns MD production at 328 K under constant pressure of 1 atm. Temperature and pressure coupling constants were both 1 ps.

We implemented all production MD simulations at 328K since our models are primarily based on the *Bca* UvrB thermophilic enzyme; experimental data with this enzyme was obtained at its physiologically relevant temperature in the present work and that of Jiang *et al.* (3). A 9 Å cutoff was applied to the non-bonded Lennard-Jones interactions. Long-range electrostatic interactions were treated with the Particle Mesh Ewald (PME) method (4,5). The SHAKE algorithm (6) was applied to constrain all bonds involving hydrogen atoms with relative geometrical tolerance of 10^{-5} Å. A 2 fs time step was used, and the

translational/rotational center-of-mass motion was removed every 1 ps (7).

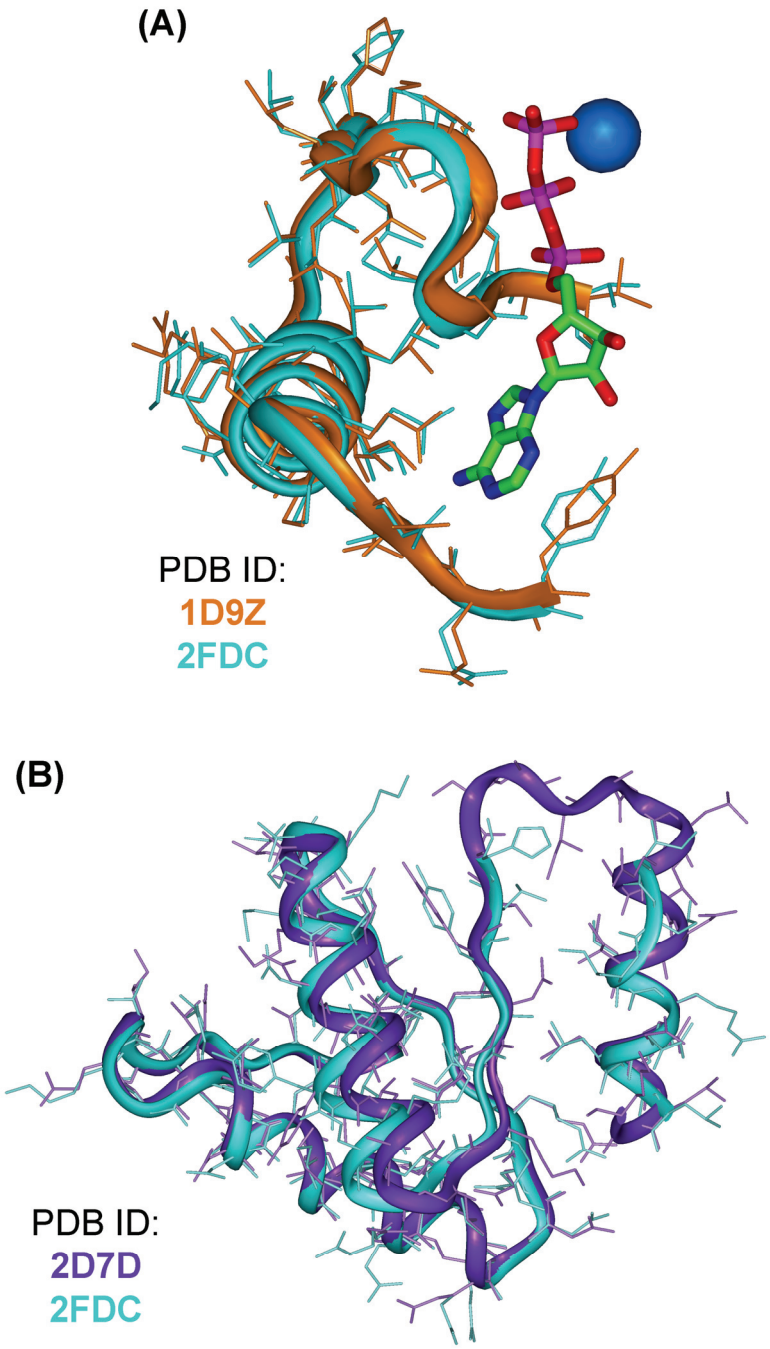

Figure S1: (A) The superimposition of the ATP binding site when modeling the ATP from 1D9Z into 2FDC. The ATP is shown in stick model colored by atom. The Mg^{2+} is shown in sphere. (B) The superimposition of protein residues 420-460 of 2FDC to residues 418-458 of 2D7D to model a missing loop from 2D7D to 2FDC. Protein is shown in cartoon with side chains shown in stick. The color code is shown in the figure.

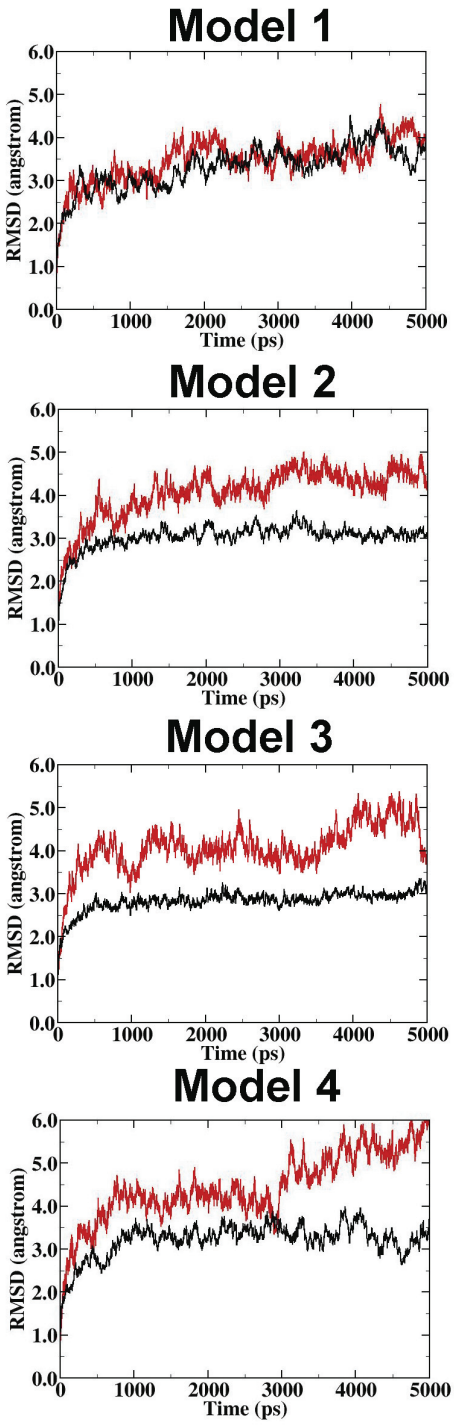

Figure S2: Plots of the all-atom root-mean-square deviations (RMSD) of the current relative to the starting structure as a function of time for the whole UvrB/DNA complex (black) and the damaged DNA (red). The damaged DNA is generally more flexible than the complex.

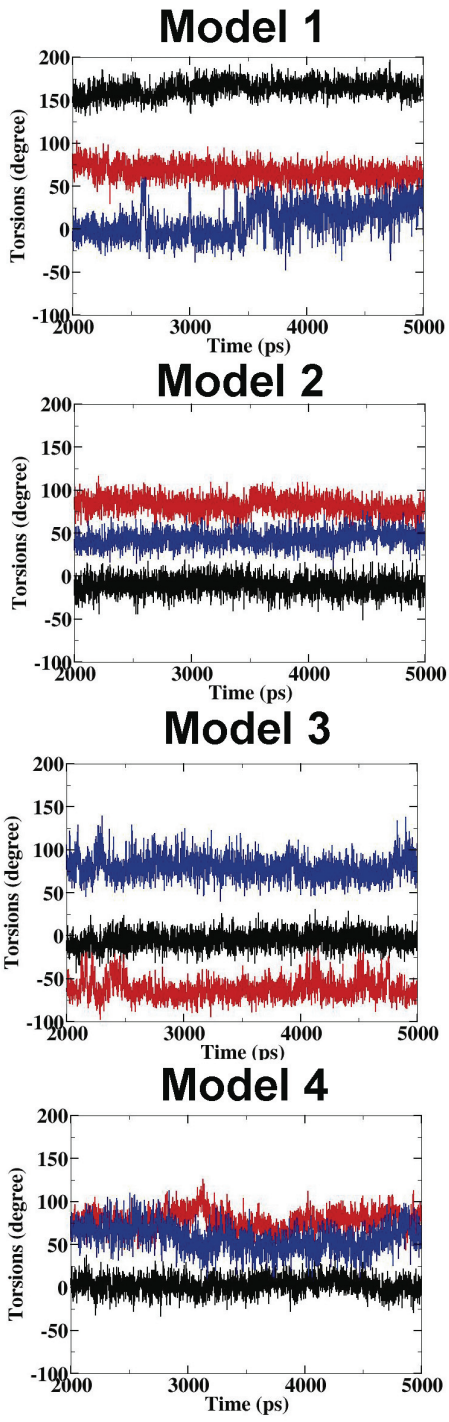

Figure S3: Plots of the torsion angles χ (blue), α' (black), and β' (red) for all complex models in the selected time frames for analysis

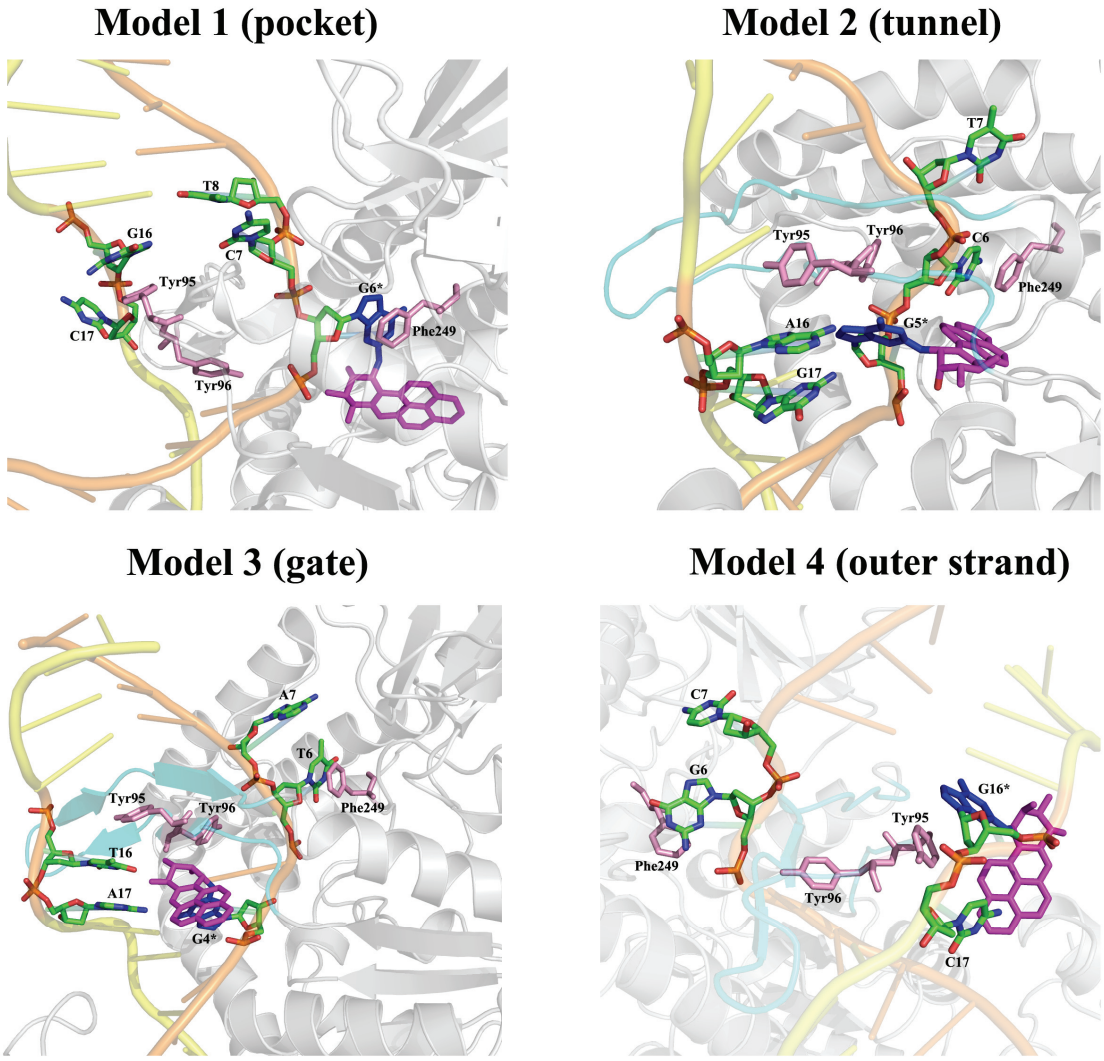

Figure S4: Flipping and stacking properties of the bases in representative structures of each model. UvrB is in cartoon and is semi-transparent. β-hairpin is shown in cyan. The G* is blue and B[*a*]P is magenta. The DNA inner strand is shown in orange and the outer strand in yellow. The bases 6, 7, 16 and 17 are shown in stick with color-coding by atom. The amino acid residues Phe249, Tyr95 and Tyr96 are shown in pink. Hydrogen atoms are deleted for clarity.

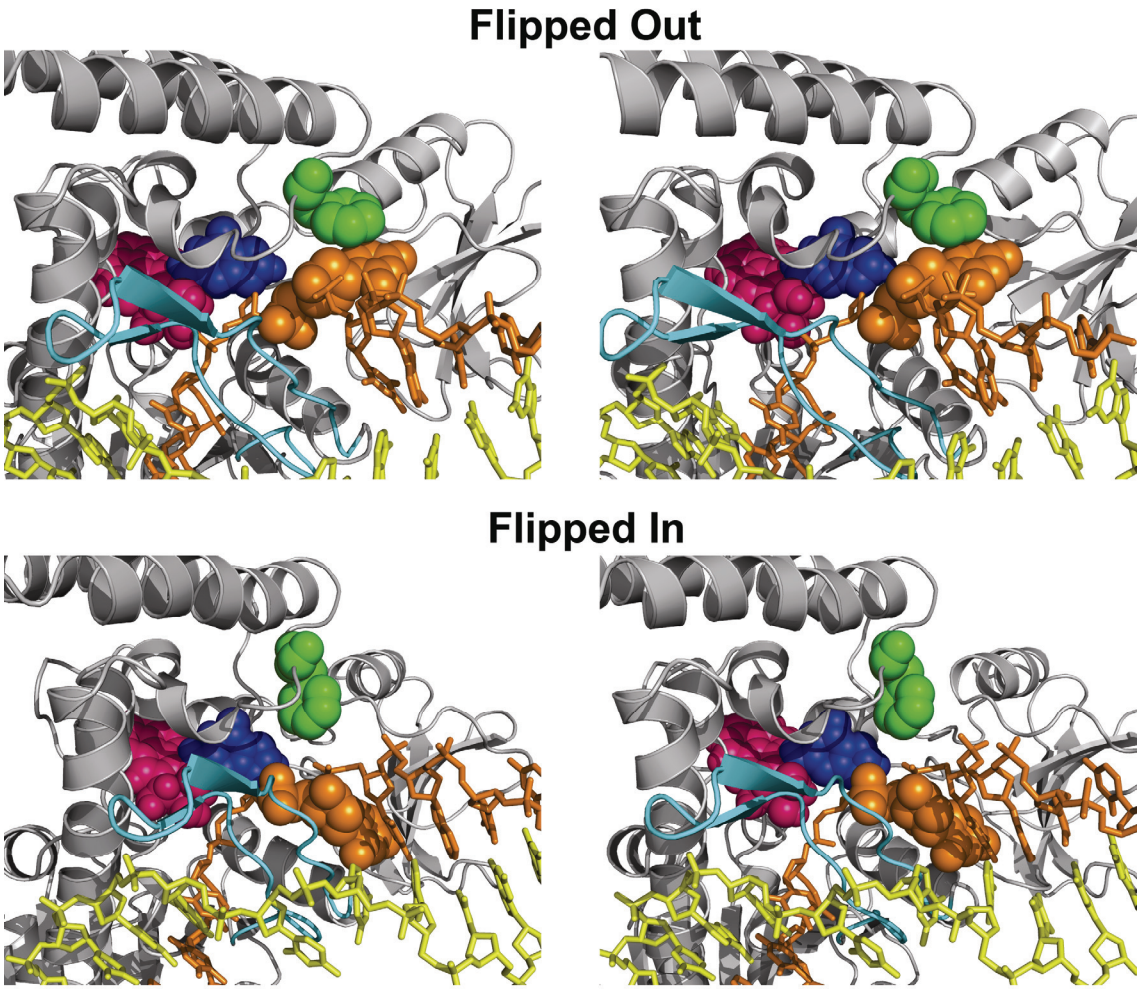

Figure S5, stereo views: The C7 base in the flipped-out and flipped-in positions of Model 1. Frames selected for illustration are at 128 ps, and 5000 ps, respectively. The C7, Phe302, and G6* are in CPK renderings. C7 is colored in orange, Phe302 is colored in green, G6* is colored in blue, and the adduct is colored in magenta. The C7 base is flipped-out in the early stage of the simulation and rotates to a flipped-in position after 1 ns of the simulation, where is remains for the duration of the simulation.

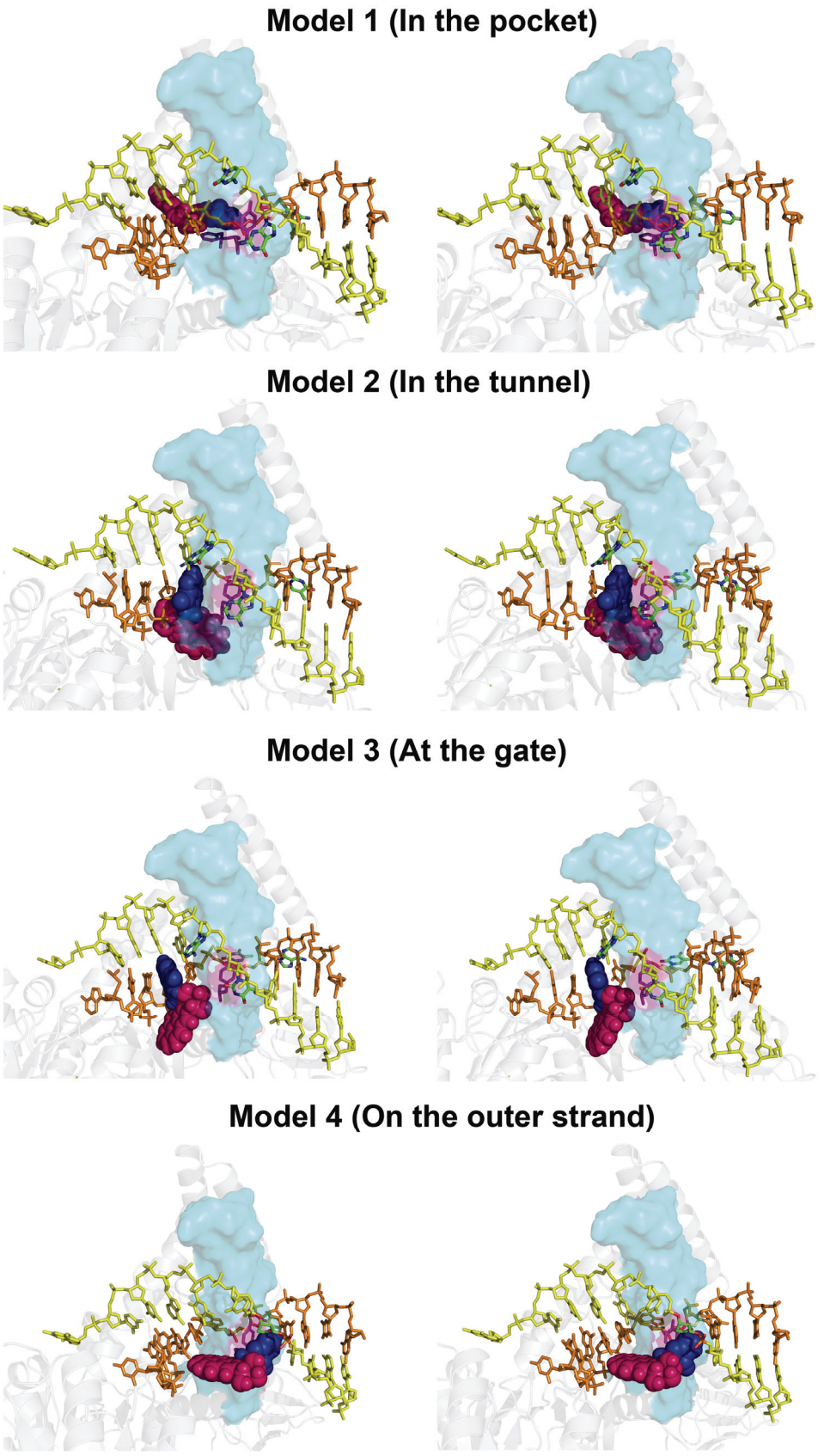

Figure S6: Stereo view of Figure 2.

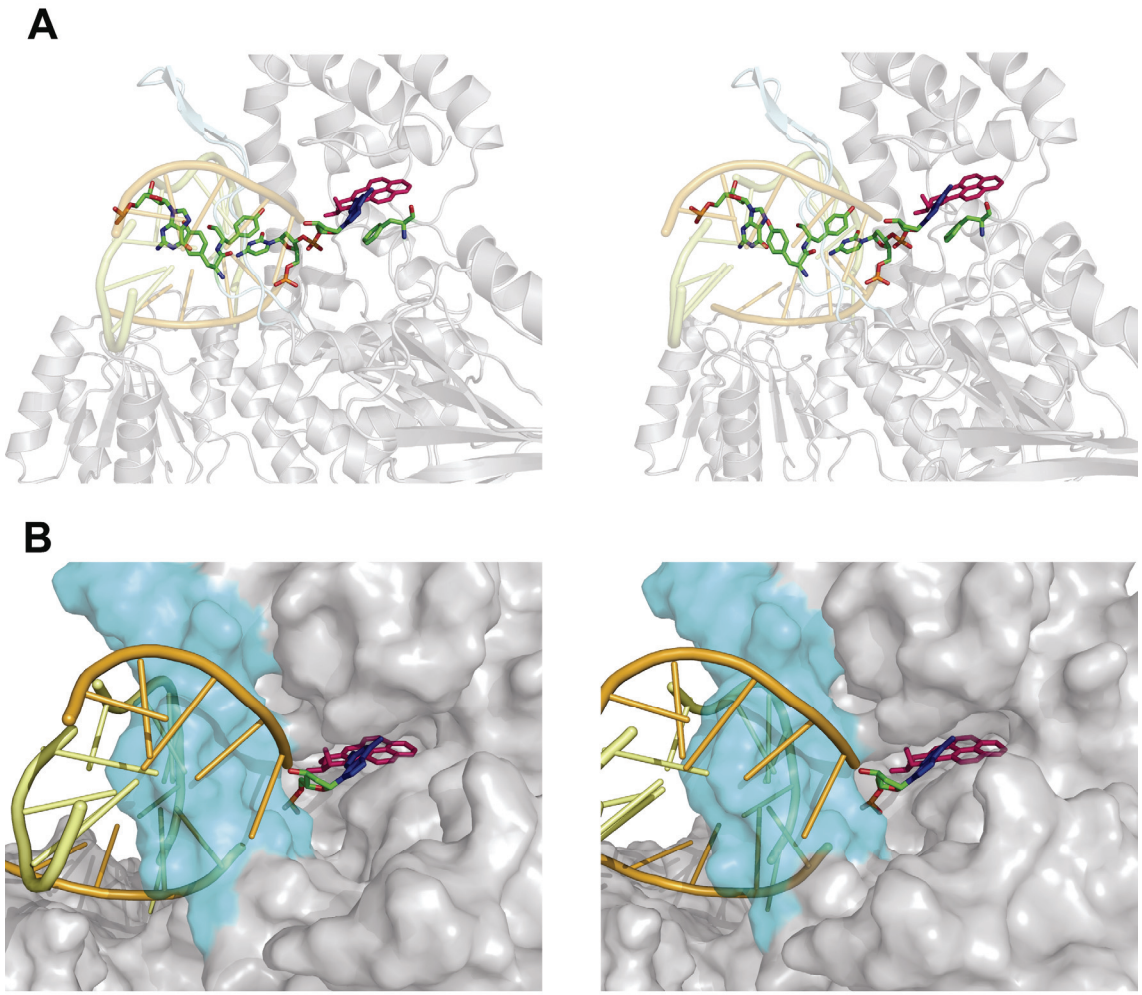

Figure S7: Stereo view of Figure 3.

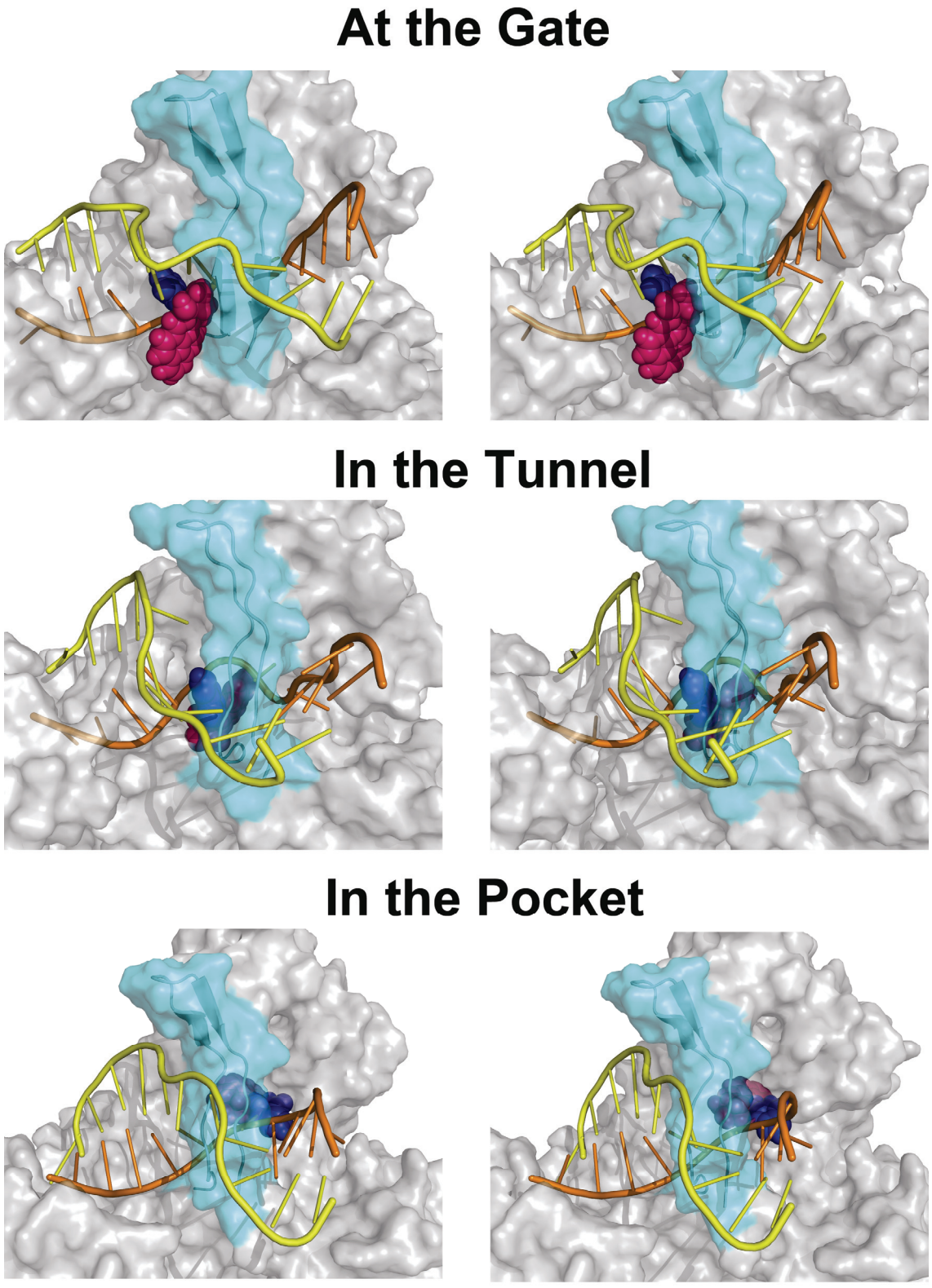

Figure S8: Stereo view of Figure 4.

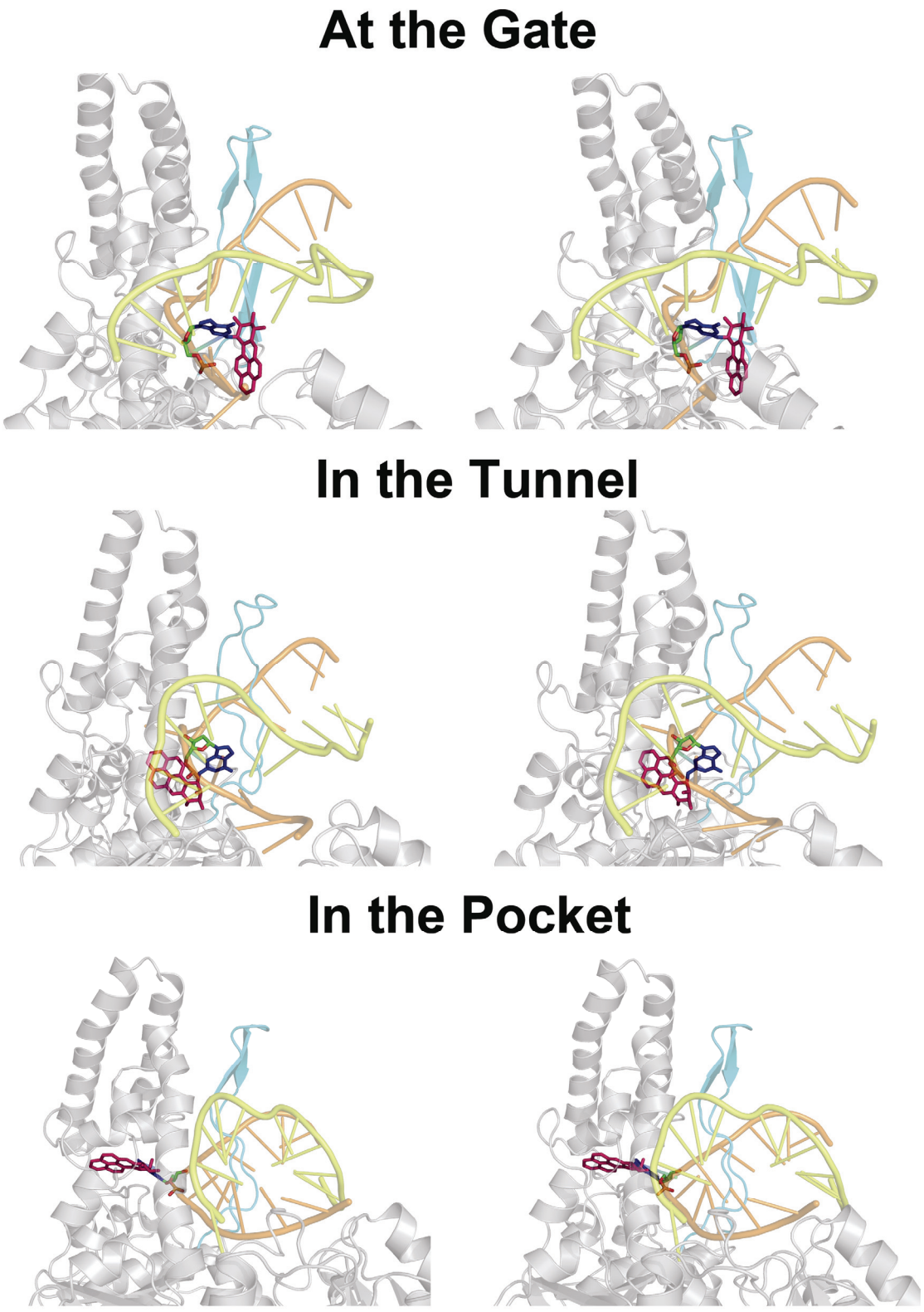

Figure S9: Stereo view Figure 4.

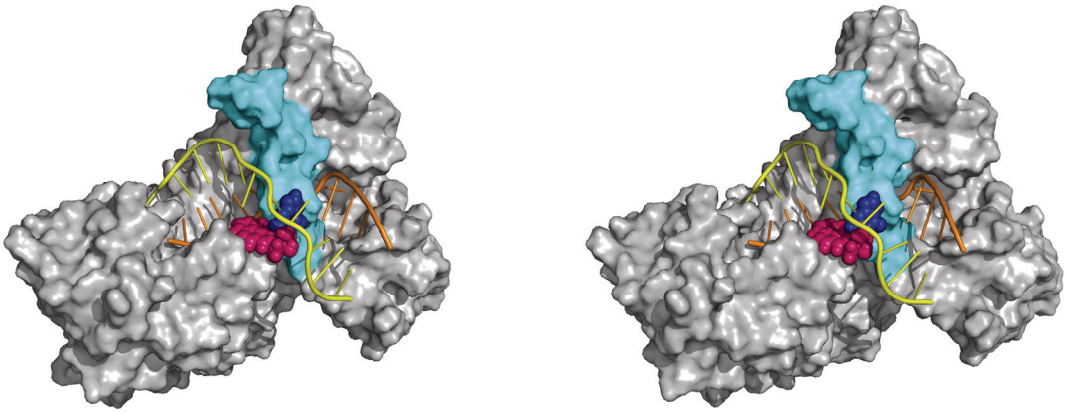

Figure S10: Stereo view Figure 5.

Table S1: Glycosidic torsion χ values in initial models for MD simulations

	χ	**α'**	**β'**
Model 1	-33°	169°	39°
Model 2	78°	63°	-29°
Model 3	61°	-64°	26°
Model 4	126°	40°	70°

Table S2: AMBER atom type, connection type, and partial charge assignments for the B[*a*]P adduct.

Atom name	Atom type	Connection type	Partial charge
P	P	M	1.218646
O1P	O2	E	-0.79319
O2P	O2	E	-0.79319
O5'	OS	M	-0.47064
C5'	CT	M	0.073767
H5'1	H1	E	0.019769
H5'2	H1	E	0.019769
C4'	CT	M	0.389993
H4'	H1	E	0.031951
O4'	OS	E	-0.30042
C3'	CT	M	-0.00134
H3'	H1	E	0.067506
C2'	CT	3	-0.00304
H2'1	HC	E	0.035953
H2'2	HC	E	0.035953
C1'	CT	B	0.096204
H1'	H2	E	0.07063
N9	N*	S	0.019725
C8	CK	B	0.024448
H8	H5	E	0.164855
N7	NB	S	-0.51017
C5	CB	S	0.183596
C6	C	B	0.416035
O6	O	E	-0.56242
N1	NA	B	-0.21083
H1	H	E	0.249318
C2	CA	B	0.086826
N3	NC	S	-0.33405
C4	CB	E	0.182261
N2	N2	B	-0.04021
H2	H	E	0.203357
C10	CT	B	-0.00353
HC10	H1	E	0.125433
CC9	CT	3	-0.02971
HC9	H1	E	0.118181
O9	OH	S	-0.5722
HO9	HO	E	0.337214
CC8	CT	3	0.331514
HC8	H1	E	0.086002

Atom name	Atom type	Connection type	Partial charge
O8	OH	S	-0.68321
HO8	HO	E	0.417026
CC7	CT	3	0.083526
HC7	H1	E	0.071384
O7	OH	S	-0.62942
HO7	HO	E	0.407107
C6A	CA	S	-0.00111
CC6	CA	B	-0.1538
HC6	HA	E	0.174033
C5A	CA	B	0.001065
C17	CA	E	0.007701
CC5	CA	B	-0.14937
HC5	HA	E	0.145695
CC4	CA	B	-0.20343
HC4	HA	E	0.156203
C3A	CA	B	0.071641
C16	CA	E	0.095343
CC3	CA	B	-0.19416
HC3	HA	E	0.166654
CC2	CA	B	-0.18043
HC2	HA	E	0.167265
CC1	CA	B	-0.15982
HC1	HA	E	0.155534
C15	CA	S	0.009637
C12	CA	B	-0.18392
HC12	HA	E	0.164501
C11	CA	B	-0.09819
HC11	HA	E	0.047767
C14	CA	S	-0.00277
C13	CA	E	-0.13559
O3'	OS	M	-0.53085

Table S3: AMBER atom type, connection type, and partial charge assignments for ATP

Atom name	Atom type	Connection type	Partial charge
O1G	O2	M	-0.98988
PG	P	M	1.361617
O2G	O2	E	-0.98988
O3G	O2	E	-0.98988
O3B	OS	M	-0.68922
PB	P	M	1.285387
O1B	O2	E	-0.78907
O2B	O2	E	-0.78907
O3A	OS	M	-0.44729
PA	P	M	0.895664
O1A	O2	E	-0.75085
O2A	O2	E	-0.75085
O5'	OS	M	-0.44344
C5'	CT	M	-0.01252
H5'1	H1	E	0.114044
H5'2	H1	E	0.114044
C4'	CT	M	0.082282
H4'	H1	E	0.012335
O4'	OS	E	-0.3307
C3'	CT	M	0.552523
H3'	H1	E	0.03123
O3'	OH	S	-0.71927
H3T	HO	E	0.379231
C2'	CT	M	0.042298
H2'	H1	E	0.115413
O2'	OH	S	-0.64696
H2T	HO	E	0.34967
C1'	CT	M	-0.0099
H1'	H2	E	0.110974
N9	N*	M	0.06168
C8	CK	M	0.113645
H8	H5	E	0.215497
N7	NB	M	-0.56702
C5	CB	M	0.033375
C4	CB	M	0.370085
N3	NC	M	-0.70756
C2	CQ	M	0.552357
H2	H5	E	0.037524
N1	NC	M	-0.84816
C6	CA	M	0.761045
N6	N2	B	-0.92335
H61	H	E	0.401472
H62	H	E	0.401472

Table S4: AMBER atom type, connection type, and partial charge assignments for Mg^{2+}

Atom name	Atom type	Connection type	Partial charge
MG	MG	M	2.000

Table S5: Box sizes and numbers of waters and counterions in MD simulation initial models

Model 1	112Å x 77Å x 96Å 18789 H_2O, 38 Na^+
Model 2	112Å x 79Å x 96Å 19441 H_2O, 38 Na^+
Model 3	112Å x 79Å x 96Å 19446 H_2O, 38 Na^+
Model 4	112Å x 77Å x 96Å 19091 H_2O, 38 Na^+

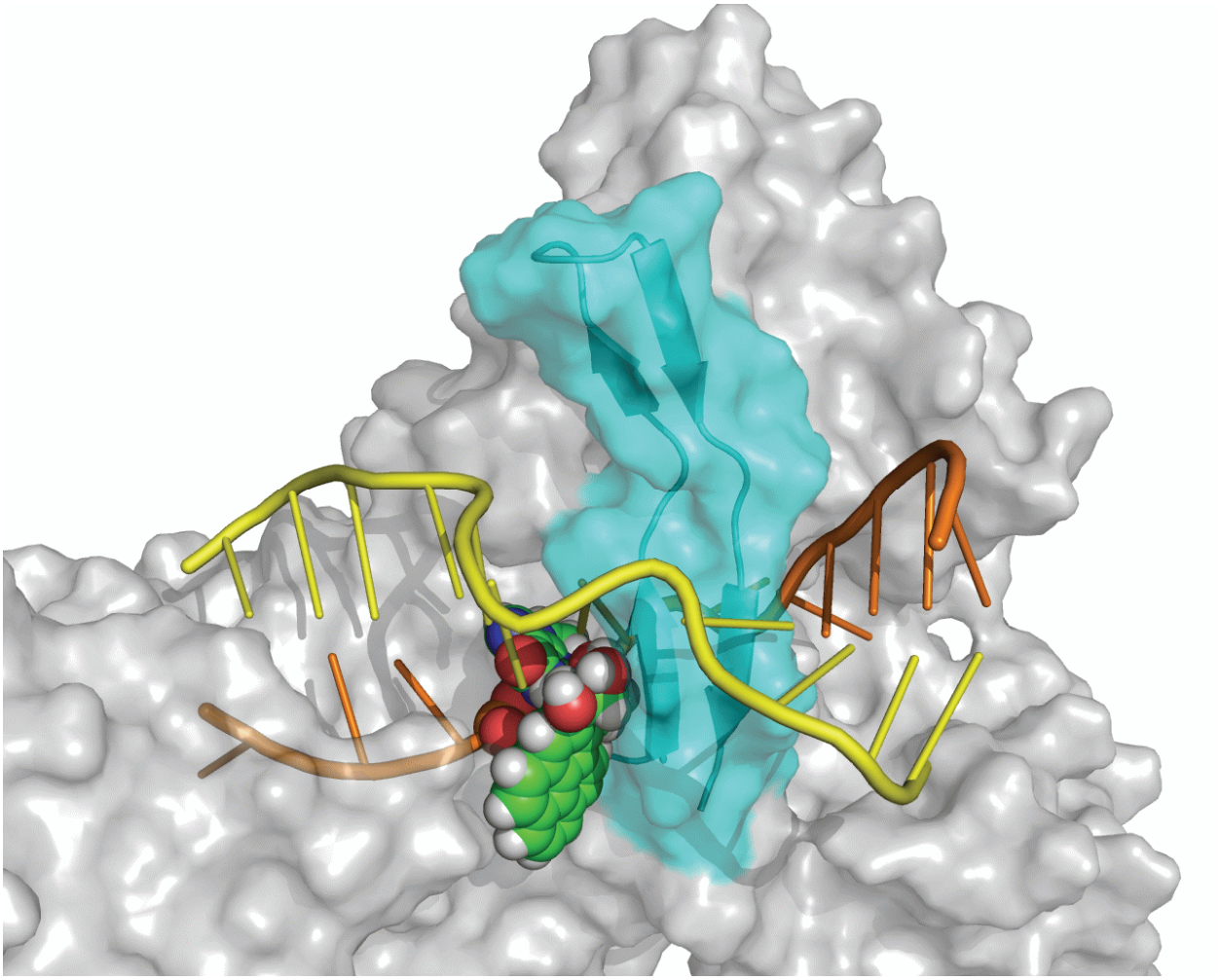

Translocation movie: The B[*a*]P lesion is in CPK colored by atom. The β-hairpin of UvrB is in cyan.

References

1. Mezei, M. (1997) Optimal position of solute for simulations. *Journal of Computational Chemistry*, **18**, 812-815.
2. Jorgensen, W.L., Chandrasekhar, J., Madura, J.D., Impey, R.W. and Klein, M.L. (1983) Comparison of Simple Potential Functions for Simulating Liquid Water. *J Chem Phys*, **79**, 926-935.
3. Jiang, G.H., Skorvaga, M., Croteau, D.L., Van Houten, B. and States, J.C. (2006) Robust incision of Benoz[a]pyrene-7,8-dihyrodiol-9,10-epoxide-DNA adducts by a recombinant thermoresistant interspecies combination UvrABC endonuclease system. *Biochemistry*, **45**, 7834-7843.
4. Darden, T., York, D. and Pedersen, L. (1993) Particle Mesh Ewald - an N.Log(N) Method for Ewald Sums in Large Systems. *J Chem Phys*, **98**, 10089-10092.
5. Essmann, U., Perera, L., Berkowitz, M.L., Darden, T., Lee, H. and Pedersen, L.G. (1995) A Smooth Particle Mesh Ewald Method. *J Chem Phys*, **103**, 8577-8593.
6. Ryckaert, J.P., Ciccotti, G. and Berendsen, H.J.C. (1977) Numerical-Integration of Cartesian Equations of Motion of a System with Constraints - Molecular-Dynamics of N-Alkanes. *J. Comput. Phys.*, **23**, 327-341.
7. Harvey, S.C., Tan, R.K.Z. and Cheatham, T.E. (1998) The flying ice cube: Velocity rescaling in molecular dynamics leads to violation of energy equipartition. *J. Comput. Chem.*, **19**, 726-740.